

Comparative Performance of Finetuned ImageNet Pre-trained Models for Electronic Component Classification

Yidi Shao

*School of Information Science and Technology
Fudan University
Shanghai, China
20307130311@fudan.edu.cn*

Longfei Zhou

*Dept. of Biomedical, Industrial and Systems Engineering
Gannon University
Erie, USA
zhou009@gannon.edu*

Fangshuo Tang

*Reading Academy
University of Reading
Reading, UK
bc804894@student.reading.ac.uk*

Xinyi Shi

*School of Pharmacy
Shanghai Jiao Tong University
Shanghai, China
clotho@sjtu.edu.cn*

Dalang Chen

*School of Business
Hubei University
Hubei, China
202121112010893@stu.hubei.edu.cn*

Shengtao Xia

*School of Architecture
Architectural Association School of Architecture
London, UK
shengtao.steven.xia@gmail.com*

Abstract—Electronic component classification and detection are crucial in manufacturing industries, significantly reducing labor costs and promoting technological and industrial development. Pre-trained models, especially those trained on ImageNet, are highly effective in image classification, allowing researchers to achieve excellent results even with limited data. This paper compares the performance of twelve ImageNet pre-trained models in classifying electronic components. Our findings show that all models tested delivered respectable accuracies. MobileNet-V2 recorded the highest at 99.95%, while EfficientNet-B0 had the lowest at 92.26%. These results underscore the substantial benefits of using ImageNet pre-trained models in image classification tasks and confirm the practical applicability of these methods in the electronics manufacturing sector.

Keywords—*electronic component, machine learning, convolutional neural network, image classification.*

I. INTRODUCTION

Electronic component class detection plays a vital role in many fields at all stages. For example, in the manufacture of electronic equipment, the accurate identification of electronic component categories in various parts of the circuit board can help check the device layout errors, improve the accuracy of production and product quality. In the maintenance and inspection of electronic equipment, correctly identifying the categories of electronic components can help to quickly locate the devices that need to be replaced or inspected, thereby reducing maintenance costs and extending the life of the

equipment [1]. In short, the class detection of electronic components can greatly save labor costs in related fields, improve the performance of electronic systems, and help promote the development of industry and technology [2], [3].

In industrial production, some traditional techniques for automated warehouse management are applied to the classification of electronic components. Some factories will allow operators to manually manage component categories with the assistance of human-machine interfaces when human resources match the number of products and the difficulty of identification; while in other cases, some factories will use Radio-Frequency Identification (RFID) or Near Field Communication (NFC) technology, attach RFID or NFC tags containing component identification information to each electronic component, and then use RFID or NFC readers on the production line to read the tag information for component identification.

In recent years, with the development of Machine Learning (ML), Deep Learning (DL) has made extraordinary contributions in many fields. Especially in image classification, DL has demonstrated its power and outstanding applicability: for example, Carlos Affonso et al. [4] utilized a Convolutional Neural Network (CNN) to achieve wood quality classification based on plank images, which achieved superior prediction performance over traditional classification techniques in highly complex scenes; while Akrem Sellami et al. [5] proposed a new method called MV-DNNet for spectral spatial classification of hyperspectral images, which is based on Multi-View

Deep Autoencoder (MVDAE) and Semi-Supervised Graph Convolutional Networks (SSGCN). Compared to traditional image classification methods such as the K-nearest neighbor (KNN) classifier, where the accuracy is limited by the range of the optimal distances [6], or Scale-Invariant Feature Transform (SIFT), where the accuracy is affected by the regularity of the object shape and the rotation angle [7], ML-based image classification methods are more tolerant of the complexity of external conditions, have better generalization capabilities, and are generally more efficient and accurate.

Pre-trained models are a powerful technique in the field of ML that learns generalized feature representations through initial training on large-scale datasets. Once pre-training is complete, these models can be fine-tuned or migrated to learn on specific tasks to adapt to more specific datasets or problems, thus improving performance and accelerating the training process. This approach provides a powerful tool for solving complex problems in the field of computer vision, especially in image classification. In image classification, the most commonly used dataset for model pre-training is ImageNet [8], which contains more than a million labeled images covering a thousand different classes of objects and scenes, allowing researchers to develop high-performing classification models through transfer learning in limited data environments. For example, Chiranjibi Sitaula et al. [9] achieved monkeypox virus recognition on human skin images using a variety of fine-tuned ImageNet pre-trained DL models; Khalid M. Hosny et al. [10] also presented the application of AlexNet pre-trained on this dataset to achieve the classification of skin lesions in human bodies.

Although computer vision-based technologies have strong advantages in image analysis, tasks in actual industrial scenarios have some specific challenges, such as the impact of differences in light intensity on images and the interference of background images on target device recognition. As shown in Fig. 1, all backgrounds are of the same category (i.e., no components), but their colors and pixel values vary greatly. In addition, all components in each row belong to the same category, but their background colors and brightness vary greatly. This poses a great challenge for machine learning-based image recognition.

Based on the importance of electronic component classification and the great advantages of ImageNet pre-training for image classification, the objectives of our study are to propose ML models fine-tuned and pre-trained on ImageNet that can accurately determine the categories of electronic component images, and to evaluate the performance of multiple pre-trained models for electronic component classification.

In this study, we evaluate 12 ImageNet pre-trained models (VGG-16, VGG-19, ResNet-18, AlexNet, EfficientNet-B0, MobileNet-V2, MobileNet-V3-Large, MobileVit-S, DenseNet-121, Xception, ViT-Small and ConvNext-Small) on an electronic component dataset comprising 11,106 images across 12 classes. We conduct comprehensive experiments comparing the models' performance through multiple metrics including accuracy, precision, recall, F1 score, and inference time per

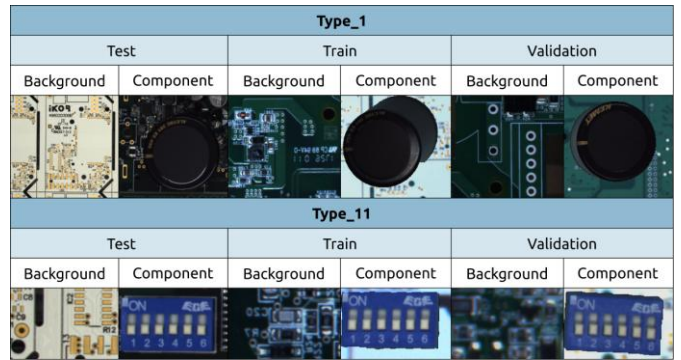


Fig. 1. Dataset structure

image, enabling a more informed selection for electronic component classification tasks in practical applications.

II. DATASET

A. Data Source

The electronic component dataset used for this study was created by Ikor as part of an industrial project carried out at Vicomtech. The objective of the project was to detect electronic components mounted on electronic boards.

In the original dataset, each of the 11 folders corresponds to a different type of electronic component. Each folder for each component type contains a training, a validation, and a test folder, and each folder contains background and component images. The images in training and validation folders are virtually generated, while those in test folders are real images. Fig. 1 illustrates the dataset structure and several sample images. Specifically, it presents examples from the 1st and 11th categories of electronic component folders. The remaining nine categories follow a similar structure and content.

B. Data Pre-processing

From the situation of the current dataset, although the folders of each class contain the backgrounds of the circuit boards deployed with the components of that class, the difference between the background boards of different classes is very unclear and each background board contains multiple components, so it is difficult to classify the background boards of different classes. So, we decided to merge all the background images and set the classification rule for electronic component images as follows: there are 12 classes, which contain 1 class of background images and 11 classes of electronic component images. In addition, there are some obvious problems with the current dataset: firstly, there is an uneven distribution of images among the test, train, and validation sets, with visibly distinct differences in the images contained in these three sets, and this can have a significant impact on training process; secondly, the ratio of images in the train, test, and validation sets is approximately 4:1:1, which is not an optimal proportion for ML in image classification; thirdly, the pixel sizes of images for each electronic component vary, and they do not conform

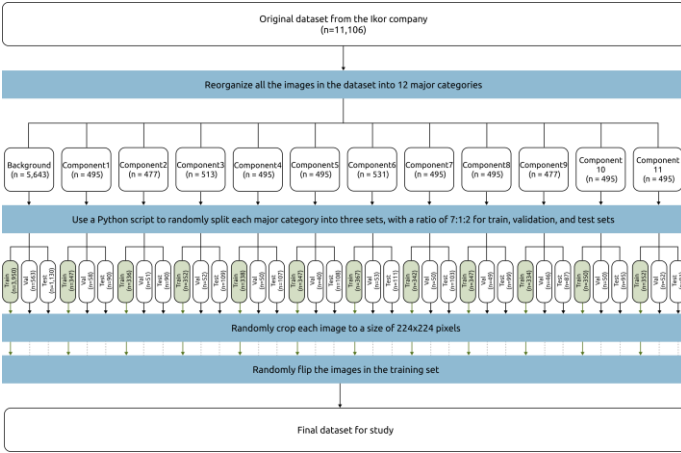


Fig. 2. Flow chart of the dataset processing steps

to the image size requirement of 224×224 pixels used in many models.

To address the above problems, we preprocessed the dataset, and the specific processing steps can be seen in the flowchart in Fig. 2. In Fig. 2, the white boxes show the results of the dataset before and after the processing steps, the blue boxes indicate the dataset processing steps, and the green arrows and dotted lines indicate that only the train sets in each class were processed with random flipping (random seed = 348), while the remaining sets were not subjected to this operation. The final dataset consists of 11,106 images. The background class contains 5,643 images, while each of the remaining 11 component classes contains approximately 500 images. Each class is divided into training, validation, and test sets with a ratio of 7:1:2. The random cropping and random flipping of the images in the train set is a kind of data enhancement, which can improve the model's ability to adapt to different scenes.

III. METHODS

A. Pre-trained Models

We chose 12 DL models pre-trained on ImageNet for this study. The models we chose are VGG-16, VGG-19, ResNet-18, AlexNet, EfficientNet-B0, MobileNet-V2, MobileNet-V3-large, MobileNet-V2, DenseNet-121, Xception, ViT-small and ConvNeXt-small. A brief discussion of each pre-trained DL model is presented in the next subsections.

1) *VGG*: The Visual Geometry Group (VGG) model is a classical CNN architecture. The VGG-16 model we use is named after its 16 layers with learnable weight parameters, including 13 convolutional layers and 3 fully connected layers [11]. VGG-19 has 3 more convolutional layers, so it has 19 layers with learnable weight parameters. Their architectures are shown in Fig. 3. VGG's deep structure benefits feature extraction, but its large number of parameters increases the risk of overfitting, especially on small datasets.

2) *AlexNet*: AlexNet, designed by Alex Krizhevsky et al., is a CNN architecture that enables multi-GPU training, which

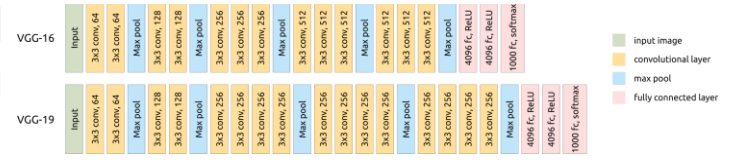


Fig. 3. VGG-16 architecture and VGG-19 architecture



Fig. 4. AlexNet architecture

supports larger models and significantly reduces training times [12]. It won the 2012 ImageNet Large Scale Visual Recognition Challenge, achieving an error rate of 15.3%, substantially better than the second place's 26.2% [13]. The network comprises 5 convolutional layers and 3 fully-connected layers [12], totaling 8 layers with learnable weights. Its architecture is detailed in Fig. 4. AlexNet's architecture was pioneering, but its limited depth compared to other models may compromise its ability to capture complex features.

3) *ResNet*: Contrary to popular belief, adding more layers to a deep network can lead to performance degradation due to vanishing gradients. To combat this, researchers have introduced skip connections and Residual Blocks (Res-Blocks), which allow networks to bypass unnecessary activations, maintaining performance [14]. In our study, we use ResNet-18, which consists of four Res-Blocks (each with four convolutional layers), an initial 7×7 convolutional layer and a fully connected layer, totaling 18 layers with learnable parameters. The architecture is depicted in Fig. 5. The residual connections of ResNet-18 makes it ideal for classifying complex components.

4) *MobileNet*: MobileNet is a streamlined, computationally efficient CNN architecture designed for mobile vision applications [15], [16]. It utilizes Linear Bottleneck Blocks, also known as Depth-wise Separable Convolution Blocks, to reduce parameters count while maintaining functionality. These blocks typically consist of a 1×1 convolution for dimensionality reduction, a 3×3 depth-wise separable convolution for feature extraction, and a convolution for dimensionality restoration. MobileNet-V2, used in our study, features 7 Bottleneck Blocks and 3 additional convolutional layers, totaling approximately 53 layers [17]. The lightweight architecture of the MobileNet-V2 model improves efficiency, but it may compromise its performance on more complex classification tasks. MobileNet-V3 builds on V2 by introducing SE blocks, h-swish activation, and NAS-optimized architecture, improving both efficiency and representational power. It has two variants:



Fig. 5. ResNet-18 architecture



Fig. 11. ViT architecture

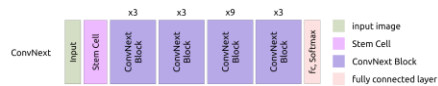


Fig. 12. ConvNeXt architecture

patch embedding, position embedding, Transformer encoders, and a classification head. Several ViT variants, including ViT-Base, ViT-Huge, ViT-Large, ViT-Small, and ViT-Tiny, have been proposed to balance accuracy and computational cost. The basic model ViT-Base contains 12 transformer layers with 86M parameters, while ViT-Small and ViT-Tiny reduce model size to 22M and 5.7M parameters, respectively, making them more suitable for limited-resource settings [29]–[31]. In this study, we refer to ViT-Small, which offers a favorable trade-off between performance and efficiency. The architecture of ViT is illustrated in Fig. 11.

10) *ConvNeXt*: ConvNeXt is a modern convolutional architecture that revisits ConvNets with design principles inspired by Vision Transformers [32]. It introduces architectural innovations such as large kernel convolutions, depthwise separable convolutions, GELU activations, and LayerNorm, while maintaining the efficiency and inductive biases of traditional ConvNets. A patchify stem using a 4×4 convolution with stride 4 replaces the standard input layer, enabling non-overlapping patch extraction akin to ViTs. The network is structured into four stages of increasing depth and channel width. Several ConvNeXt variants—including ConvNeXt-Tiny, Small, Base, Large, and X-Large—have been proposed to offer flexible trade-offs between performance and complexity. In this study, we adopt ConvNeXt-Small. Its architecture is illustrated in Fig. 12 [33].

B. Implementation

We conducted our study in the PyTorch 1.11.0 Environment. We utilized 12 ImageNet pre-trained models from both the PyTorch official library (torchvision) and the timm (PyTorch Image Models) library. We used the following configurations: learning rate = $3e-5$, batch size = 64 for both train and test, and the epoch = 5. We made modifications to each model based on transfer learning: the number of output classifications was changed to 12 for the last layer, the weights of that layer were initialized, and the learning rate of that layer was changed to 10 times that of the other layers. Each of the models was optimized using Stochastic Gradient Descent (SGD) with a weight decay of 0.001.

IV. RESULTS

After training, validating, and testing the 12 models separately, the comprehensive results obtained by each of them are shown in Table I and further illustrated by the training,

validation, and testing curves in Fig. 13. To facilitate visualization and comparison, the training accuracy, training loss, and validation accuracy curves for the 12 models are grouped into sets of four in Fig. 14 to Fig. 16, avoiding overcrowding the plots. The confusion matrix heatmaps for the test set results are shown in Fig. 17. In each heatmap, the horizontal axis represents the predicted labels, while the vertical axis represents the true labels, providing a detailed breakdown of per-class performance.

In the training accuracy plot, as shown in Fig. 14, we observe varying initial performance and convergence speeds among the models. Models like ViT-Small and MobileNet-V2 start with relatively high training accuracy and quickly converge towards near-perfect accuracy within 5 epochs. AlexNet, ResNet-18, VGG-16, VGG-19, and MobileNet-V3-Large also demonstrate rapid improvement and achieve high training accuracy. In contrast, models like ConvNeXt-Small, Xception, MobileViT-S, and particularly EfficientNet-B0 exhibit significantly lower initial training accuracies, with EfficientNet-B0 starting just above 40%. However, these models, despite their low starting points, show the most substantial relative improvement over the 5 epochs, highlighting effective learning during the training phase.

The training loss plot, as shown in Fig. 15, generally mirrors the accuracy trends. All models show a consistent decrease in training loss as epochs increase. Models that started with high initial accuracy (like MobileNet-V2, ViT-Small) tend to have lower initial losses and continue to decrease steadily. ViT-Small, VGG-16, and VGG-19 achieve very low final training losses (below 0.05), indicating they fit the training data very well. Xception and EfficientNet-B0, starting with high losses, exhibit the steepest initial drop in loss, signifying significant learning progress from a poor starting state. After 5 epochs, EfficientNet-B0 still has the highest training loss (around 1.00), while Xception reaches a more respectable 0.25. This suggests EfficientNet-B0 struggled more than others to minimize loss on the training data within the given epochs.

The validation accuracy plot, as shown in Fig. 16, is crucial for assessing generalization performance on unseen data. Most models demonstrate excellent generalization, quickly reaching validation accuracies well above 99%. MobileNet-V2, VGG-16, VGG-19, and ViT-Small are among the top performers, with their validation accuracy curves closely clustered and reaching high levels rapidly. AlexNet and DenseNet-121 also perform strongly but show some minor fluctuations with slight dips before recovery. ResNet-18 shows a slightly slower initial rise compared to some models but reaches a high validation accuracy. EfficientNet-B0 significantly lags behind the others throughout validation, with its accuracy curve remaining distinctly lower and finishing just above 90%. MobileViT-S and ConvNeXt-Small, while not starting as high as some top models, also converge rapidly to high validation accuracy after around 4 epochs.

Table I presents a comprehensive comparison of the 12 models on the test set, including accuracy, precision, recall, F1 score, inference time, number of parameters, and FLOPs.

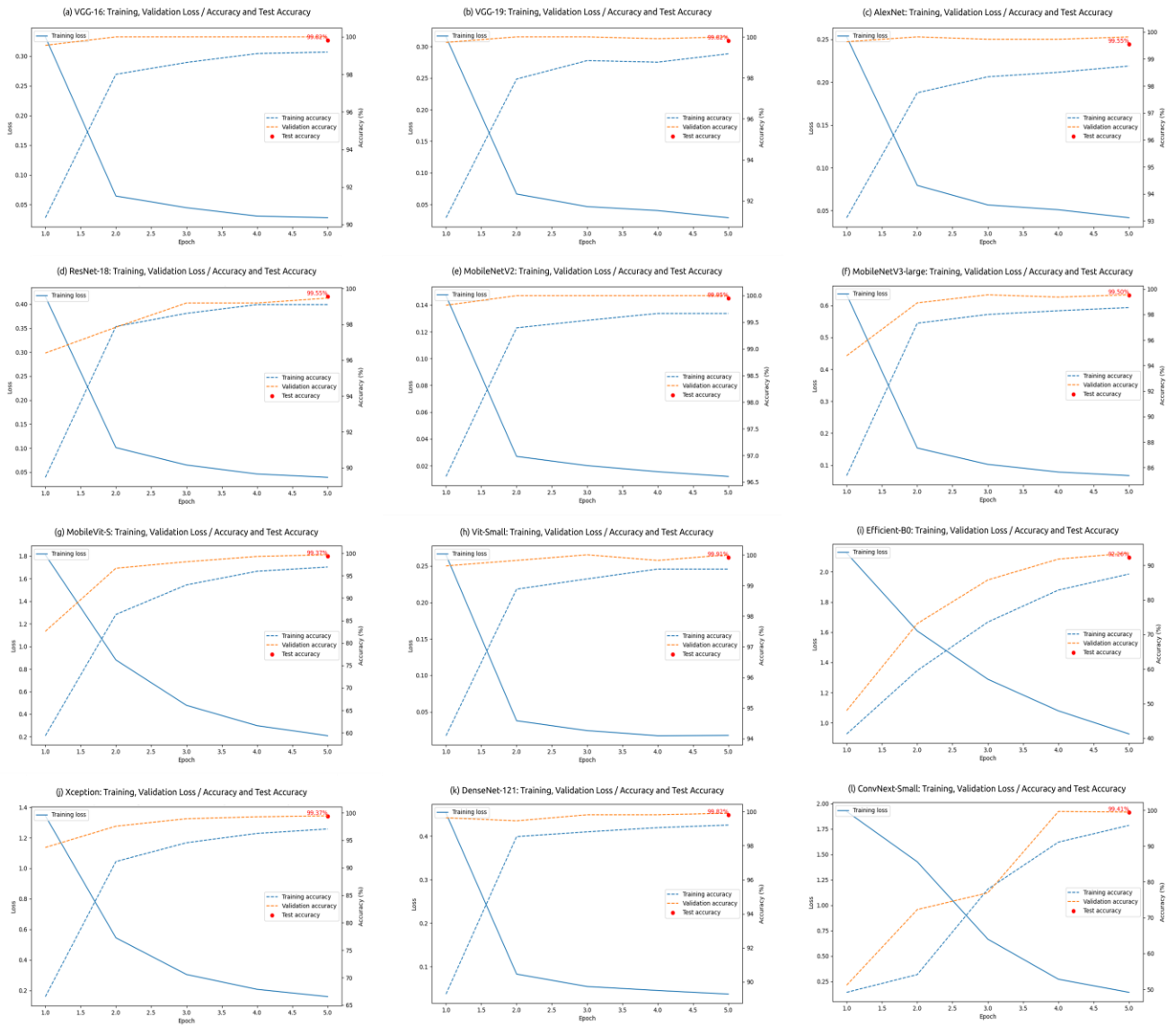


Fig. 13. Training, validation and testing results for each of the 12 models, including training loss, training accuracy, validation accuracy, and test accuracy for (l) VGG-16, (b) VGG-19, (c) AlexNet, (d) ResNet-18, (e) MobileNet-V2, (f) MobileNet-V3-Large, (g) MobileVit-S, (h) ViT-Small, (i) EfficientNet-B0, (j) Xception, (k) DenseNet-121, (l) ConvNeXt-Small

Highlighting MobileNet-V2’s performance, it stands out as the model with the best overall profile for practical application in this task. First, it achieved the highest test accuracy at 99.95%, demonstrating exceptional classification capability, with only one misclassification occurring in the background class as shown in its confusion matrix. Second, it is a remarkably lightweight model, possessing only 3.4 million parameters, which is among the smallest parameter counts of all tested models. This makes it highly suitable for deployment on devices with limited memory or computational resources, common in industrial settings. Third, its inference time per image is notably fast at 2.60 ms, enabling rapid processing necessary for real-time applications or high-throughput inspection lines. This combination of top-tier accuracy, minimal parameter footprint, and rapid inference speed positions MobileNet-V2 as the most advantageous model for real-world electronic

component classification based on our evaluation.

Examining the other models reveals various trade-offs. ViT-Small achieves nearly identical top accuracy (99.91%) and is fast (2.1 ms), but has significantly more parameters (22M) than MobileNet-V2. VGG-16 and VGG-19 also achieve high accuracy (99.82%) and decent speed (3.45ms/2.67ms), but are excessively large in terms of parameters (138M/144M), making them impractical for resource-constrained environments. DenseNet-121 (99.82% accuracy) has moderate parameters (8M) but is the slowest among the high-accuracy models (7.71ms), likely due to its dense connectivity pattern increasing computational cost during inference. AlexNet (99.55% accuracy) is very fast (1.07ms) due to its simpler architecture, but has a larger parameter count (60M) than MobileNet-V2 and slightly lower accuracy. ResNet-18 (99.55% accuracy) offers a good balance with moderate pa-

TABLE I. COMPARISON OF PERFORMANCE

Model	Test Acc (%)	Precision (%)	Recall (%)	F1 (%)	Inference Time per img (ms)	Number of Parameters	FLOPs
MobileNet-V2	99.95	99.96	99.95	99.96	2.60	3.4M	0.3G
ViT-Small	99.91	99.91	99.91	99.91	2.11	22M	4.6G
VGG-16	99.82	99.82	99.82	99.82	3.45	138M	15.5G
VGG-19	99.82	99.82	99.82	99.82	2.67	144M	19.6G
DenseNet-121	99.82	99.82	99.82	99.82	7.71	8M	2.9G
AlexNet	99.55	99.56	99.55	99.55	1.07	60M	0.7G
ResNet-18	99.55	99.55	99.55	99.54	2.16	11M	1.8G
MobileNet-V3-Large	99.50	99.52	99.50	99.51	3.12	5.4M	0.22G
ConvNeXt-Small	99.41	99.42	99.41	99.41	9.88	50M	8.7G
Xception	99.37	99.38	99.37	99.37	2.90	22M	8.4G
MobileViT-S	99.37	99.38	99.37	99.36	4.48	2.0M	2.0G
EfficientNet-B0	92.26	93.12	92.26	91.26	5.59	5.3M	0.39G
<i>MobileNet-V2*</i>	93.20	93.91	93.20	92.67	-	-	-
<i>EfficientNet-B0*</i>	82.49	74.89	82.49	77.61	-	-	-

Note: "*" indicates non-pretrained models.

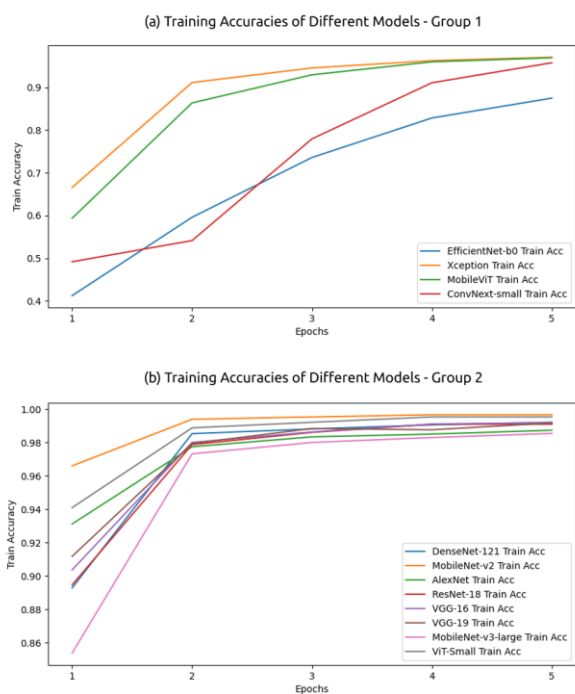


Fig. 14. Comparison of training accuracy for the 12 models, including: (a) training accuracy of EfficientNet-B0 (blue), Xception (orange), MobileViT (green), and ConvNeXt-Small (red); (b) training accuracy of DenseNet-121 (blue), MobileNet-V2 (orange), AlexNet (green), ResNet-18 (red), VGG-16 (purple), VGG-19 (brown), MobileNet-V3-Large (pink), and ViT-Small (gray)

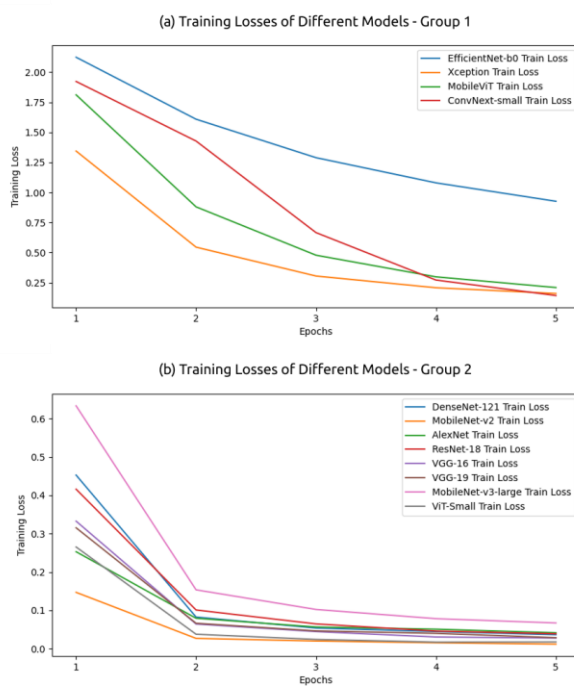


Fig. 15. Comparison of training loss for the 12 models, including: (a) training loss of EfficientNet-B0 (blue), Xception (orange), MobileViT (green), and ConvNeXt-Small (red); (b) training loss of DenseNet-121 (blue), MobileNet-V2 (orange), AlexNet (green), ResNet-18 (red), VGG-16 (purple), VGG-19 (brown), MobileNet-V3-Large (pink), and ViT-Small (gray)

rameters (11M) and decent speed (2.16ms), leveraging residual connections for depth but not achieving the peak efficiency of MobileNet-V2. MobileNet-V3-Large (99.50% accuracy) is also very lightweight (5.4M) and relatively fast (3.12ms), representing an excellent evolution of the MobileNet architecture. MobileViT-S (99.37% accuracy) is the most parameter-efficient model (2.0M) but slightly slower (4.48ms) than

MobileNet-V2. ConvNeXt-Small (99.41% accuracy) achieves high accuracy but has a large parameter count (50M) and is the slowest overall (9.88ms), indicating its architecture, while powerful, might be less efficient on this specific task/dataset compared to MobileNets. Xception (99.37% accuracy) uses depthwise separable convolutions effectively, achieving good accuracy and fast inference (2.90ms) with moderate parameters (22M). EfficientNet-B0, despite being designed for effi-

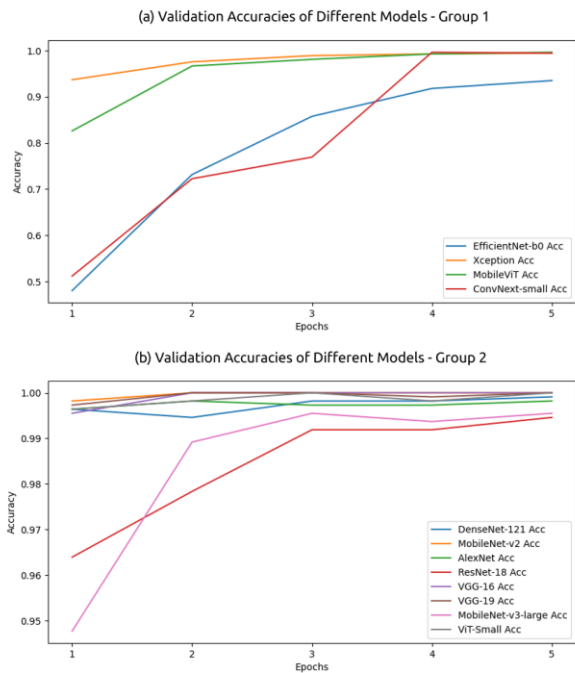


Fig. 16. Comparison of validation accuracy for the 12 models, including: (a) validation accuracy of EfficientNet-B0 (blue), Xception (orange), MobileViT (green), and ConvNeXt-Small (red); (b) validation accuracy of DenseNet-121 (blue), MobileNet-V2 (orange), AlexNet (green), ResNet-18 (red), VGG-16 (purple), VGG-19 (brown), MobileNet-V3-Large (pink), and ViT-Small (gray)

ciency through compound scaling, exhibits significantly poorer accuracy (92.26%) compared to all other models, frequently misclassifying components as background. This suggests its specific scaling strategy or architecture is not well-suited for the nuances of this dataset within the given training constraints, performing poorly despite moderate parameters (5.3M) and decent speed (5.59ms).

Moreover, to better demonstrate the benefits of the pre-training process, we also conducted classification using non-pretrained versions of MobileNet-V2 and EfficientNet-B0, which had the best and worst performance when pretrained, respectively. The results show that their test accuracies were 93.20% and 82.49%. Both models experienced a noticeable decrease in accuracy compared to their pretrained versions, highlighting that pretraining can significantly enhance the performance of models compared to their non pretrained counterparts.

V. CONCLUSIONS

In this paper, we successfully applied transfer learning with ImageNet pre-trained models to the task of electronic component classification. We conducted a comparative evaluation of twelve different state-of-the-art models on a domain-specific dataset. Our results demonstrate that high classification accuracy can be achieved with a minimal number of training epochs, underscoring the significant benefits of leveraging ImageNet pre-training for such tasks. Specifically, pre-training

provides powerful initial feature representations, accelerates convergence, and offers flexibility for adaptation to new data.

Among the evaluated models, MobileNet-V2 emerged as the most suitable choice for practical deployment in electronic manufacturing. This conclusion is based on its outstanding performance across multiple key metrics: First, it achieved the highest test accuracy of 99.95%, indicating superior classification capability. Second, it is a remarkably lightweight model with only 3.4 million parameters, making it highly efficient in terms of memory and storage requirements, crucial for resource-constrained environments. Third, it demonstrated very fast inference time per image (2.60 ms), enabling rapid processing essential for real-time inspection and high-throughput applications. This unique combination of top-tier accuracy, minimal parameter footprint, and rapid inference speed distinguishes MobileNet-V2.

While many other models also achieved excellent test accuracies above 99% (such as ViT-Small, VGG-16, VGG19, DenseNet-121, AlexNet, ResNet-18, MobileNet-V3-Large, ConvNeXt-Small, Xception, and MobileViT-S), they presented various trade-offs in terms of size and speed. For instance, VGG models were highly accurate but excessively large, DenseNet-121 was accurate but slower, and some modern architectures like ConvNeXt-Small, while powerful, were significantly slower or larger than MobileNet-V2. In stark contrast, EfficientNet-B0 exhibited notably lower accuracy (92.26%), indicating it struggled to effectively learn the specific features of this dataset compared to the other models, despite being designed for efficiency. The inclusion of non-pretrained results further highlighted the critical role of ImageNet pre-training for achieving high performance in this domain.

Limitations of our work: First, the size and potential heterogeneity of our dataset may limit the generalizability of findings. Expanding the dataset with more varied, real-world images is crucial for robust evaluation. Second, while ImageNet pre-training is powerful, domain shifts might still require more targeted fine-tuning or training approaches for optimal performance in all real-world scenarios. Lastly, handling proprietary data necessitates strict protocols to address privacy and data leakage concerns.

In future work, we plan to expand our comparison of classification techniques. Additionally, we aim to conduct deeper analysis of model performance using methods such as feature importance and error analysis. We also intend to expand our dataset to better reflect real-world conditions, improving model generalizability. Lastly, we will address ethical concerns, including potential biases and privacy risks related to proprietary data, by establishing stricter data handling protocols and ensuring transparency in data collection.

REFERENCES

- [1] L. Zhou, L. Zhang, and N. Konz, "Computer vision techniques in manufacturing," *IEEE Transactions on Systems, Man, and Cybernetics: Systems*, vol. 53, no. 1, pp. 105–117, 2022.
- [2] F. Teng *et al.*, "A new convolutional neural network for identification of damaged electronic components," in *2022 6th International Conference on Universal Village (UV)*. IEEE, 2022, pp. 1–6.

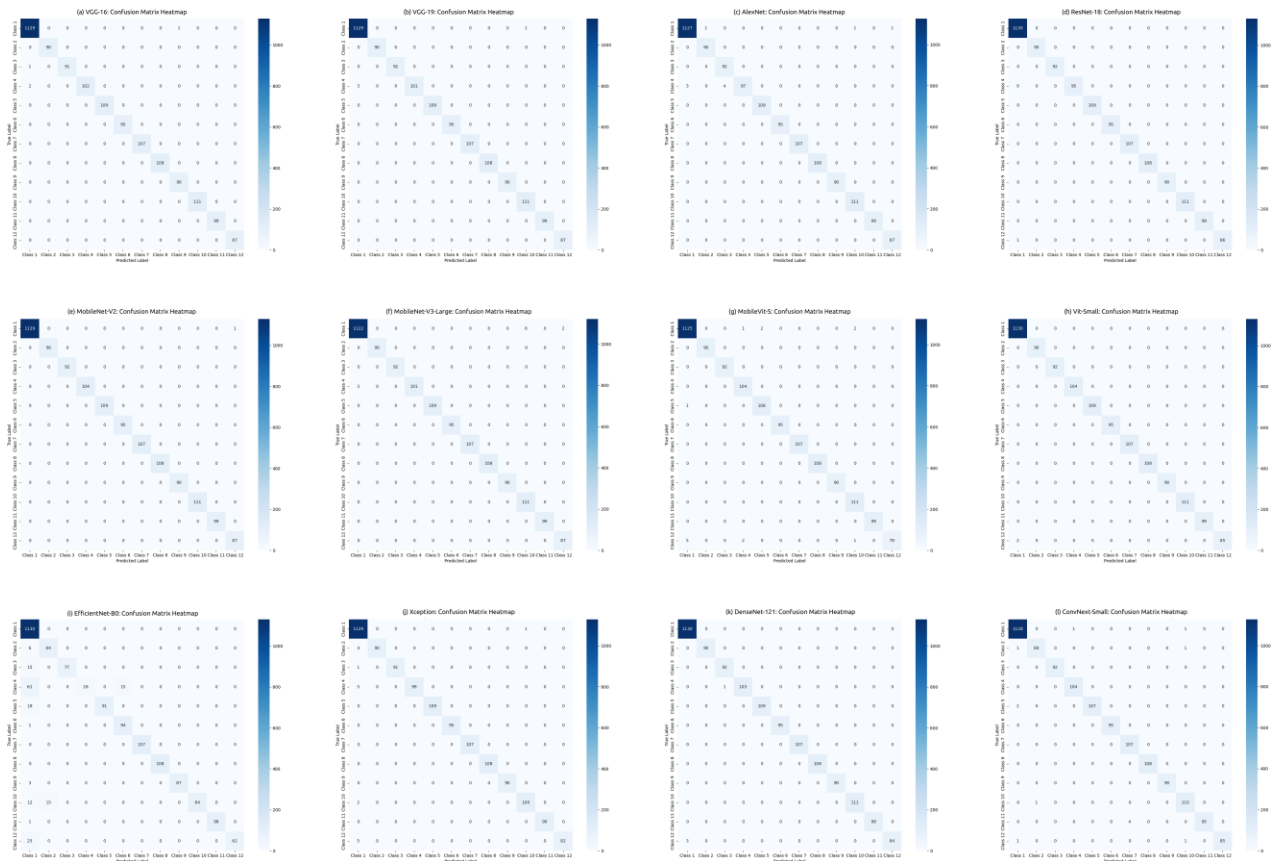


Fig. 17. Comparison of Confusion Matrix Heatmap for the 12 models, including: (1) VGG-16, (b) VGG-19, (c) AlexNet, (d) ResNet-18, (e) MobileNet-V2, (f) MobileNet-V3-Large, (g) MobileViT-S, (h) ViT-Small, (i) EfficientNet-B0, (j) Xception, (k) DenseNet-121, (l) ConvNeXt-Small

- [3] L. Zhou and L. Zhang, "A novel convolutional neural network for electronic component classification with diverse backgrounds," *International Journal of Modeling, Simulation, and Scientific Computing*, vol. 13, no. 01, p. 2240001, 2022.
- [4] C. Affonso, A. L. D. Rossi, F. H. A. Vieira, A. C. P. de Leon Ferreira *et al.*, "Deep learning for biological image classification," *Expert systems with applications*, vol. 85, pp. 114–122, 2017.
- [5] A. Sellami and S. Tabbone, "Deep neural networks-based relevant latent representation learning for hyperspectral image classification," *Pattern Recognition*, vol. 121, p. 108224, 2022.
- [6] H. A. Abu Alfeilat *et al.*, "Effects of distance measure choice on k-nearest neighbor classifier performance: a review," *Big data*, vol. 7, no. 4, pp. 221–248, 2019.
- [7] W. Setiawan, A. Wahyudin, and G. Widiyanto, "The use of scale invariant feature transform (sift) algorithms to identification garbage images based on product label," in *2017 3rd international conference on science in information technology (ICSITech)*. IEEE, 2017, pp. 336–341.
- [8] J. Deng *et al.*, "Imagenet: A large-scale hierarchical image database," in *2009 IEEE conference on computer vision and pattern recognition*. Ieee, 2009, pp. 248–255.
- [9] C. Sitaula and T. B. Shahi, "Monkeypox virus detection using pre-trained deep learning-based approaches," *Journal of Medical Systems*, vol. 46, no. 11, p. 78, 2022.
- [10] K. M. Hosny, M. A. Kassem, and M. M. Foad, "Skin cancer classification using deep learning and transfer learning," in *2018 9th Cairo international biomedical engineering conference (CIBEC)*. IEEE, 2018, pp. 90–93.
- [11] S. Mascarenhas and M. Agarwal, "A comparison between vgg16, vgg19 and resnet50 architecture frameworks for image classification," in *2021 International conference on disruptive technologies for multi-disciplinary research and applications (CENTCON)*, vol. 1. IEEE, 2021, pp. 96–99.
- [12] A. Krizhevsky, I. Sutskever, and G. E. Hinton, "Imagenet classification with deep convolutional neural networks," *Advances in neural information processing systems*, vol. 25, 2012.
- [13] J. Deng *et al.*, "Imagenet large scale visual recognition competition 2012 (ilsvrc2012)," *See net.org/challenges/LSVRC*, vol. 41, p. 6, 2012.
- [14] X. Ou *et al.*, "Moving object detection method via resnet-18 with encoder–decoder structure in complex scenes," *IEEE Access*, vol. 7, pp. 108 152–108 160, 2019.
- [15] A. G. Howard *et al.*, "Mobilenets: Efficient convolutional neural networks for mobile vision applications," *arXiv preprint arXiv:1704.04861*, 2017.
- [16] H. Nguyen, "Fast object detection framework based on mobilenetv2 architecture and enhanced feature pyramid," *J. Theor. Appl. Inf. Technol*, vol. 98, no. 05, 2020.
- [17] M. Sandler, A. Howard, M. Zhu, A. Zhmoginov, and L. C. Chen, "Mobilenetv2: Inverted residuals and linear bottlenecks," in *Proceedings of the IEEE conference on computer vision and pattern recognition*, 2018, pp. 4510–4520.
- [18] A. Howard *et al.*, "Searching for mobilenetv3," in *Proceedings of the IEEE/CVF international conference on computer vision*, 2019, pp. 1314–1324.
- [19] C. Nwaneto and C. Yinka-Banjo, "Harnessing deep learning algorithms for early plant disease detection: A comparative study and evaluation between ssd (mobilenet_v2 and mobilenet_v3) and cnn model," *Ife Journal of Science*, vol. 26, no. 3, pp. 555–568, 2024.
- [20] M. Tan and Q. Le, "Efficientnet: Rethinking model scaling for convolutional neural networks," in *International conference on machine learning*. PMLR, 2019, pp. 6105–6114.

- [21] M. UC, an, B. Kaya, and M. Kaya, "Multi-class gastrointestinal images classification using efficientnet-b0 cnn model," in *2022 International Conference on Data Analytics for Business and Industry (ICDABI)*. IEEE, 2022, pp. 1–5.
- [22] B. TOPTAS, and D. HANBAY, "The separation of glaucoma and non-glaucoma fundus images using efficientnet-b0," *Bitlis Eren U niversitesi Fen Bilimleri Dergisi*, vol. 11, no. 4, pp. 1084–1092, 2022.
- [23] M. A. Moid and M. A. Chaurasia, "Transfer learning-based plant disease detection and diagnosis system using xception," in *2021 Fifih International Conference on I-SMAC (IoT in Social, Mobile, Analytics and Cloud)(I-SMAC)*. IEEE, 2021, pp. 1–5.
- [24] G. P. Kanna *et al.*, "Advanced deep learning techniques for early disease prediction in cauliflower plants," *Scientific Reports*, vol. 13, no. 1, p. 18475, 2023.
- [25] S. A. Albelwi, "Deep architecture based on densenet-121 model for weather image recognition," *International Journal of Advanced Computer Science and Applications*, vol. 13, no. 10, 2022.
- [26] S. Mehta and M. Rastegari, "Mobilevit: light-weight, general-purpose, and mobile-friendly vision transformer," *arXiv preprint arXiv:2110.02178*, 2021.
- [27] A. Wang, H. Chen, Z. Lin, J. Han, and G. Ding, "Repvit: Revisiting mobile cnn from vit perspective," in *Proceedings of the IEEE/CVF Conference on Computer Vision and Pattern Recognition*, 2024, pp. 15 909–15 920.
- [28] P. Sun, H. Zhang, J. Yang, and D. Wei, "Mobilevit based lightweight model for prohibited item detection in x-ray images," in *Asian Conference on Pattern Recognition*. Springer, 2023, pp. 45–58.
- [29] A. Dosovitskiy, "An image is worth 16x16 words: Transformers for image recognition at scale," *arXiv preprint arXiv:2010.11929*, 2020.
- [30] H. Touvron *et al.*, "Training data-efficient image transformers & distillation through attention," in *International conference on machine learning*. PMLR, 2021, pp. 10 347–10 357.
- [31] J. Ling *et al.*, "Patient teacher can impart locality to improve lightweight vision transformer on small dataset," *Pattern Recognition*, vol. 157, p. 110893, 2025.
- [32] Z. Liu *et al.*, "A convnet for the 2020s," in *Proceedings of the IEEE/CVF conference on computer vision and pattern recognition*, 2022, pp. 11 976–11 986.
- [33] S. B. Yengec-Tasdemir, Z. Aydin, E. Akay, S. Dogan, and B. Yilmaz, "Improved classification of colorectal polyps on histopathological images with ensemble learning and stain normalization," *Computer Methods and Programs in Biomedicine*, vol. 232, p. 107441, 2023.